

Symposium of the International Society for Rock Mechanics

## Cylindrical Cavity Deformation of Jointed Anisotropic Rock Masses. Empirical Approach

M. Muñoz-Menéndez<sup>a\*</sup>, A. Perucho-Martínez<sup>a</sup>, M.J. Rodríguez-Peces<sup>b</sup>, H. Cano-Linares<sup>a</sup><sup>a</sup>Laboratorio de Geotecnia, CEDEX. Alfonso XII,3-5, Madrid 28024, Spain<sup>b</sup>Departamento de Geodinámica, Universidad Complutense de Madrid. Jose Antonio Novais,12, Madrid 28040, Spain

---

### Abstract

Interpretations of cavity expansion tests (pressuremeter, radial jack, etc.) are based (in most occasions) on the analysis of the deformability of a cylindrical cavity in a continuous, isotropic, and homogeneous medium. However, many rock masses show an anisotropic behaviour due to the presence of discontinuity planes of different origins. Cavity expansion tests in these media have been studied here with an empirical approach. Several tests have been simulated in a three-dimensional, anisotropic and discontinuous medium—using 3DEC by Itasca—and their deformation has been analyzed in order to establish the principal factors that control the behaviour of the rock mass in these situations. Based on this analysis, it has been developed a new method for the interpretation of the cavity expansion tests carried out in laminated rock masses, which allows estimating the principal deformation moduli of the rock mass (maximum and minimum). This method can be used for any dip of the discontinuity planes.

© 2017 The Authors. Published by Elsevier Ltd. This is an open access article under the CC BY-NC-ND license

(<http://creativecommons.org/licenses/by-nc-nd/4.0/>).

Peer-review under responsibility of the organizing committee of EUROCK 2017

**Keywords:** Cavity expansion; pressuremeter; deformability; anisotropy; joints; discontinuous media

---

### 1. Introduction

The deformation modulus of the rock mass is one of the most important parameters for a geotechnical engineering project. The determination of this parameter is an issue not completely solved, neither from a theoretical nor from a practical point of view [1, 2].

---

\* Corresponding author. Tel.: +34 91-335-7384; fax: +34 91-335-7322.

E-mail address: [mauro.muniz@cedex.es](mailto:mauro.muniz@cedex.es)

Most of the existing field testing methods for the measure of the deformability are expensive and hard to place. Among these methods, pressuremeter test is the easiest and the least expensive one. The interpretation of this test is based on the cavity expanding theory in a continuous and isotropic medium but, most of rock masses are anisotropic and discontinuous media due to the presence of bedding or joint planes. Because of this, the usual interpretation of pressuremeter tests must be questioned, reviewed and, probably, a new methodology must be proposed.

### 1.1. Theoretical background

As it has been mentioned, the habitual interpretation of pressuremeter tests supposes a homogeneous, continuous and isotropic medium with a radial symmetry. According to the cavity expanding theory, the pressuremeter modulus ( $E_p$ ) can be obtained from the analysis of the load-deformation diagram:

$$E_p = R_m \frac{\Delta P}{\Delta R} (1 + \nu) \quad (1)$$

where  $E_p$ : pressuremeter modulus;  $\Delta P$ : applied load increment;  $\Delta R$ : radius increment;  $R_m$ : average radius on elastic zone;  $\nu$ : Poisson's ratio.

During the inflation of the pressuremeter, the central axis of the probe does not always remain centered on the borehole. The displacement of this axis makes the radial displacement measures useless so only the diametric displacements can be used for deformation determinations.

The most habitual elastic models in rock mechanics are the lineal isotropy and the transverse isotropy; however a rock mass with a discontinuity set (e.g. bedding, jointing or foliation) can be analyzed with another model: the transverse isotropy due to discontinuity planes. In this model, the deformability of the medium is the sum of the deformability of the intact rock (lineal isotropic) and the deformability of the layers. Using this model, the deformability of the rock mass ( $E_c$  and  $G_c$ ) can be calculated as follows [3]:

$$\frac{1}{E_c} = \frac{1}{E_i} + \frac{1}{\lambda \cdot k_n} \quad (2)$$

$$\frac{1}{G_c} = \frac{1}{G_i} + \frac{1}{\lambda \cdot k_s} \quad (3)$$

where  $E_c$ : deformation modulus of the rock mass;  $E_i$ : deformation modulus of the intact rock;  $\lambda$ : joint spacing;  $k_n$ : normal stiffness of the joints;  $G_c$ : shear modulus of the rock mass;  $G_i$ : shear modulus of the intact rock;  $k_s$ : shear stiffness of the joints.

The deformability of an expanding cylindrical cavity in an anisotropic medium has been studied by several authors [4-7], but none of them has taken into account the phenomena due to the presence of discontinuities and, most of them, are useful only for specific orientations of the layers in relation with the cavity [4, 6]. A rigorous method has not been found [7]. Some authors have studied the deformability of excavated cavities (e.g. tunnels) in anisotropic media [8-11], only two of them take into account the presence of discontinuities [9, 10]. Fortsakis et al. [9] conclude that the use of a continuous model for the analysis of a jointed medium underestimates the deformation. Wang and Huang [10] highlight the importance of the phenomena of joint slide in the deformation of these media.

## 2. Methods

### 2.1. Scale effect

As exposed in Fortsakis et al. [9], the numerical modelling of a rock mass with anisotropy due to discontinuities can be made by two methods (Fig. 1): as an equivalent anisotropic medium calculated by Eq. 2 and 3; or as an isotropic medium (intact rock) and discontinuity planes (joints). Fortsakis et al. [9] analyzed the differences between these two methods in the estimation of the deformation of a rock mass due to the excavation of a tunnel.

Muñiz Menéndez [12] studied this phenomenon in the case of radial load. According to this author, these two methods may differ depending on the ratio between joint spacing ( $\lambda$ ) and cavity radius ( $R$ ). For  $\lambda/R \leq 0.4$  the two methods give similar results but, for  $\lambda/R > 0.4$  only the discontinuous model is applicable.

### 2.2. Model

In this study, we considered different dips ( $\beta$ ) of the discontinuity planes (from 0 to 90°), together with a ratio  $\lambda/R > 0.4$ , so we decided to use a discontinuous model. We performed the calculi with the 3D distinct element code 3DEC (4.11.066 version) by Itasca [13]. This software combines finite differences for the intact rock and discontinuous elements for the discontinuities.

The model's geometry consisted in a square prism (2 x 2 x 3 m) crossed by a cylindrical cavity (100 mm diameter) centered in the bases. The pressuremeter probe was simulated by a radial load in the center of the cavity with a length of 500 mm. A load of 10 MPa was applied in all cases.

For the modelling of the discontinuities we adopted a Mohr-Coulomb criterion with no-dilatancy, and a persistence greater than the model. For the intact rock, we considered a linear elastic, isotropic, and homogeneous model. Fig. 2 shows a scheme of the model. Fig. 3 shows an example of the calculi.

The geotechnical parameters shown in Table 1 were adopted from Muñiz Menéndez [12] and they correspond to the Algeciras Unit (Spain).  $E_i$ ,  $\nu$ ,  $k_s$ ,  $c_j$ , and  $\phi_j$  were obtained through laboratory tests;  $\lambda$ ,  $k_n$  and  $\sigma_{1,2,3}$  were estimated. In some calculi, we modified these parameters for the study of the influence of each of them. We suppose a  $k_n$  constant with the deformation.

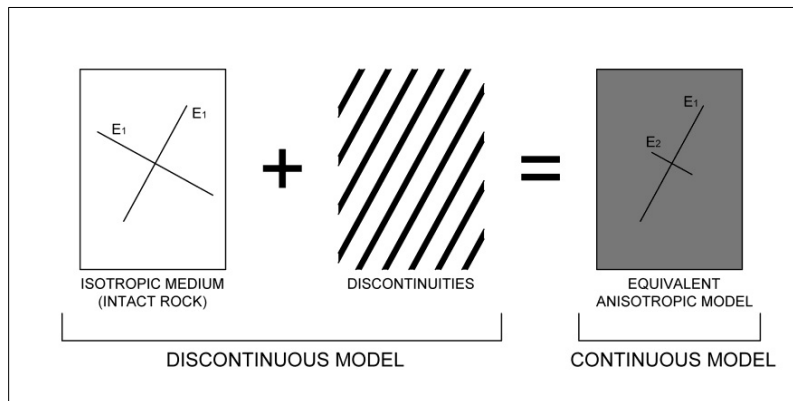


Fig. 1. Different anisotropic models. Modified from Fortsakis et al. [9].

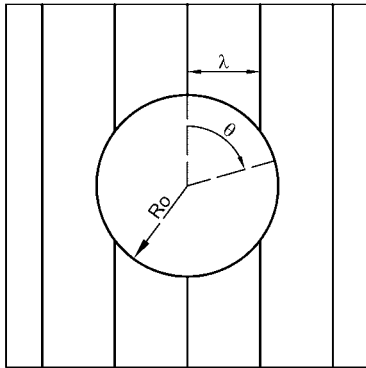


Fig. 2. Model scheme. Horizontal cross section.

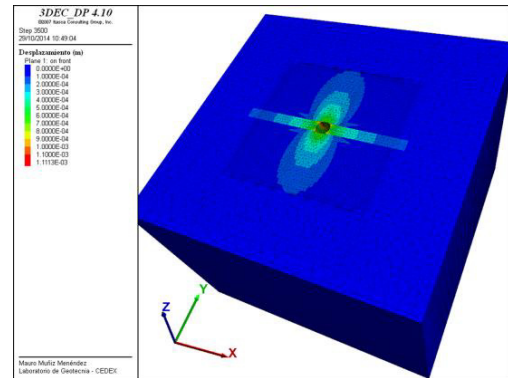
Fig. 3. 3DEC model with  $\beta=80^\circ$ . Horizontal cross section.

Table 1. Model's reference parameters.

Deformation modulus of the intact rock	$E_i$	4500 MPa
Poisson's ratio of the intact rock	$\nu$	0.28
Joints spacing	$\lambda$	0.04 m
Normal stiffness of the joints	$k_n$	50 GPa/m
Shear stiffness of the joints	$k_s$	0.8 GPa/m
Cohesion of the joints	$c_j$	0.4 MPa
Friction angle of the joints	$\phi_j$	$18^\circ$
Isotropical stress field	$\sigma_1=\sigma_2=\sigma_3$	3 MPa

### 3. Results and discussion

For each combination of parameters, we made 10 calculations, varying the dip angle of the joint planes from  $0^\circ$  to  $90^\circ$ . Radial displacements were measured in 24 points (separated by  $15^\circ$ ), situated in the center of the loading zone. We made more than 90 simulations in total. Fig. 4 to 6 show some of the results of radial displacements and they make evident the influence of different parameters ( $\beta$ ,  $E_i$ ,  $k_n$ ).

#### 3.1. The critical angle $\chi$

Fig. 4 shows a critical angle from which a “jump” exists in the curve ( $\Delta R-\theta$ ). This “jump” is due to the slide of the discontinuity planes. This critical angle ( $\chi$ ) depends on the ratio  $\lambda/R_0$  (joint spacing / initial radius for the cavity) according to Eq. 4:

$$\chi = \arcsin \left( \frac{\lambda}{R_0} \right) \quad (4)$$

Fig. 5 and 6 show a clear influence of both the deformability of the intact rock ( $E_c$ ) and the normal stiffness of the joints ( $k_n$ ) on the deformability of the rock mass ( $E_c$ ).

The  $\chi$  angle is defined as: the dip angle from which the apparent joint spacing in the measurement plane is equal to the radius of the borehole. For dip angles greater than  $\chi$ , the load applied is transmitted parallel to the joints direction, involving one or more of them (red zone in Fig. 7) which can slide due to the inexistence of continuity

in both sides of the hole. For dip angles lower than  $\chi$ , these beds continue to both side of the hole (blue in Fig. 7) avoiding the slide.

Consequently, the interpretation of these tests must be made in two ways: one way for  $\beta < \chi$ , and another way for  $\beta > \chi$ .

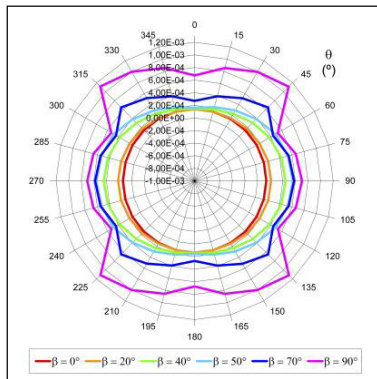


Fig. 4. Influence of dip in the deformation of cylindrical cavity. Radial load of 10 MPa.

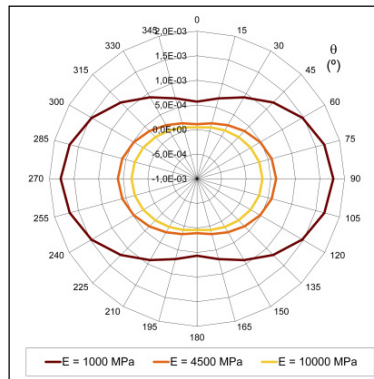


Fig. 5. Influence of  $E_I$  in the deformation of cylindrical cavity. Radial load of 10 MPa.

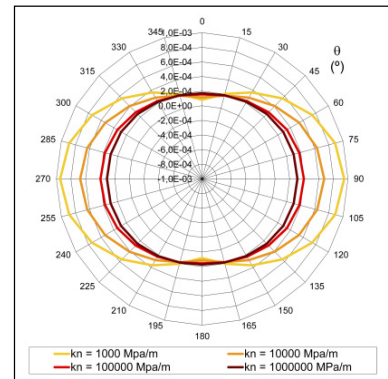


Fig. 6. Influence of  $k_n$  in the deformation of cylindrical cavity. Radial load of 10 MPa.

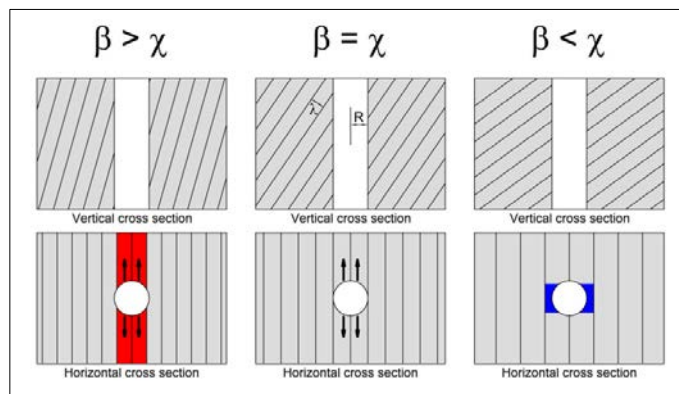


Fig. 7. Variation of the behavior of a cylindrical cavity in fissured medium with  $\beta$ - $\chi$  ratio.

### 3.2. Deformation when $\beta < \chi$

For dip angles lower than  $\chi$ , the curve “ $\Delta R$ - $\theta$ ” can be approximated following the Eq. 5:

$$\Delta R_{\theta} = \Delta R_{0^{\circ}} \cdot \left[ 1 + \sin^2 \beta \cdot \sin^2 \theta \cdot \sin \chi \cdot (1 + 2\nu) \cdot \frac{E_{0^{\circ}}}{E_{90^{\circ}}} \right] \quad (5)$$

where:

$$\Delta R_{0^{\circ}} = (1 + \nu) R_0 \frac{\Delta P}{E_{0^{\circ}}} \cdot \left[ 1 + \left( \frac{\beta - \chi/2}{150} \right) \right] \quad (6)$$

After analyzing the results, we observed that the radial displacement estimated parallel to the discontinuities ( $\Delta R_{0^\circ}$ ) is greater than the theoretical one (Eq. 1) proposed by most authors [4]. Fig. 8 to 10 show the deformation calculated with 3DEC and the deformation estimated with the proposed equations.

### 3.3. Deformations when $\beta > \chi$

When dip angles are greater than  $\chi$ , a “jump” is observed in the diagram “ $\Delta R$ - $\theta$ ” (Fig. 11). This “jump” occurs at  $\theta = \chi/\sin(\beta)$ .

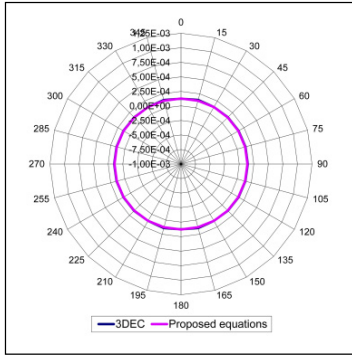


Fig. 8. Deformations calculated with 3DEC and with empirical equations for  $\beta = 10^\circ$ .

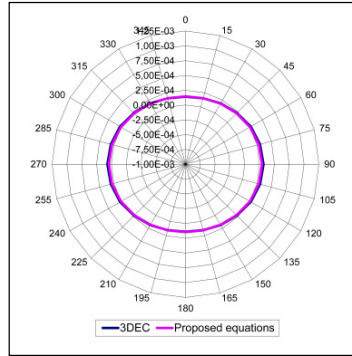


Fig. 9. Deformations calculated with 3DEC and with empirical equations for  $\beta = 30^\circ$ .

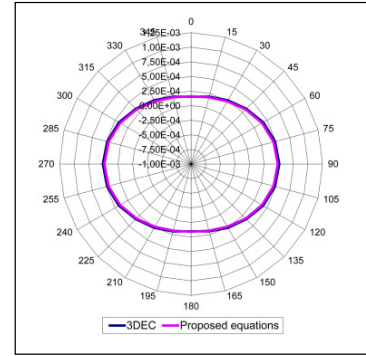


Fig. 10. Deformations calculated with 3DEC and with empirical equations for  $\beta = 45^\circ$ .

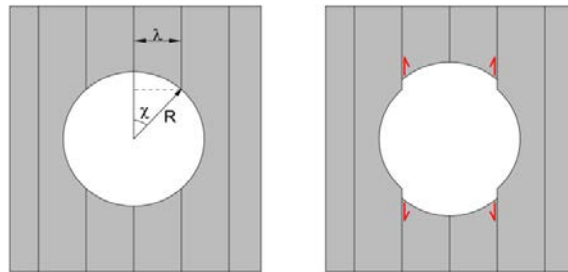


Fig. 11. Behavior of a radial loaded cylindrical cavity in a fissured medium with  $\beta > \chi$ .

When  $\chi/\sin(\beta) < \theta \leq 90^\circ$ , radial displacements are lower than those observed when  $\beta < \chi$ . These radial displacements can be approximated by a modification of Eq. 5 as is proposed in Eq. 7.

$$\Delta R_\theta = \Delta R_{0^\circ} \left[ 1 + \sin^2 \beta \cdot \sin^2 \theta \cdot \sin \chi \cdot (1 + 2\nu) \cdot \frac{E_{0^\circ}}{E_{90^\circ}} \right] - \Delta R' \quad (7)$$

where, in this case:

$$\Delta R' = \Delta R_{0^\circ} \left[ \sin \chi \cdot \sin \beta \left( \frac{k_s}{4000 \text{ MPa/m}} + 1.66 \right) \right] \quad (8)$$

when  $\chi/\sin(\beta) > \theta$ , radial displacements can be calculated by Eq. 7, but adding the displacement produced for the “jump” ( $\Delta R_\chi$ ) as is shown in Eq. 9.

$$\Delta R_\theta = \Delta R_{0^\circ} \left[ 1 + \sin^2 \beta \cdot \sin^2 \theta \cdot \sin \chi \cdot (1 + 2\nu) \cdot \frac{E_{0^\circ}}{E_{90^\circ}} \right] - \Delta R' + \Delta R_\chi \quad (9)$$

This “jump” ( $\Delta R_\chi$ ) can be estimated, in this model, with Eq. 10.

$$\Delta R_\chi = \Delta R_{0^\circ} \left[ 2 \cdot (1 + \nu) \cdot \lambda \cdot (\beta - 45^\circ) \cdot \frac{11250 \text{ MPa/m} - k_s}{12500 \text{ MPa/m}} \right] \quad (10)$$

Fig. 12 to 14 show the results calculated when  $\beta > \chi$  with 3DEC and with the proposed empirical equations.

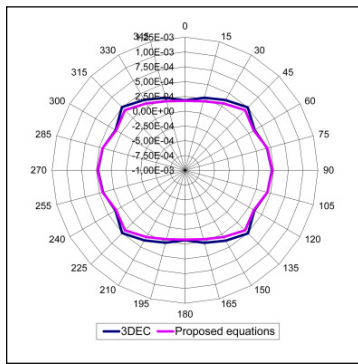


Fig. 12. Deformations calculated with 3DEC and with empirical equations for  $\beta = 60^\circ$ .

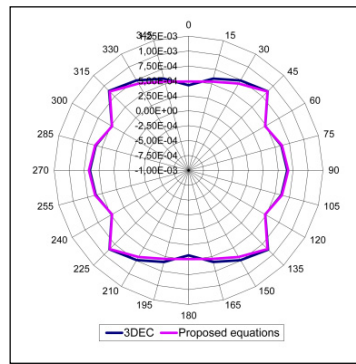


Fig. 13. Deformations calculated with 3DEC and with empirical equations for  $\beta = 80^\circ$ .

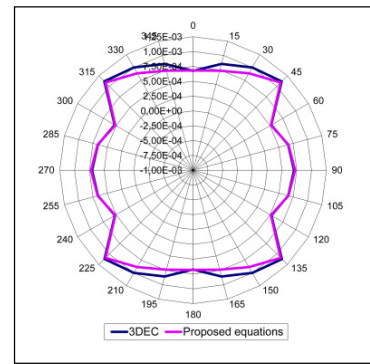


Fig. 14. Deformations calculated with 3DEC and with empirical equations for  $\beta = 90^\circ$ .

Using the equations above, the deformation parameter of the rock mass can be estimated with the analysis of pressuremeter tests for any dip of the discontinuity sets.

### 3.4. Comparison with other methods

In order to compare the proposed equation with some of the methods proposed by other authors (see paragraph 1.1), we have calculated the same example with each methodology (Fig. 15) using parameters from Table 1 and  $\beta = 90^\circ$ . The ratio  $R_0/\lambda$  was equal to 0.8.

According to this study, it seems that some continuous methods either underestimate the deformation of the cavity, particularly parallel to horizontal traces [4, 5]; or overestimate the deformation, particularly perpendicular to horizontal traces [6].

The method proposed in this paper shows the best fit to the model calculated with 3DEC, and it is the only one that predicts the slide of the joints. The method we proposed is useful for the estimation of the deformation of a cylindrical cavity in a jointed rock mass and, therefore, for the interpretation of pressuremeter tests in this kind of media.



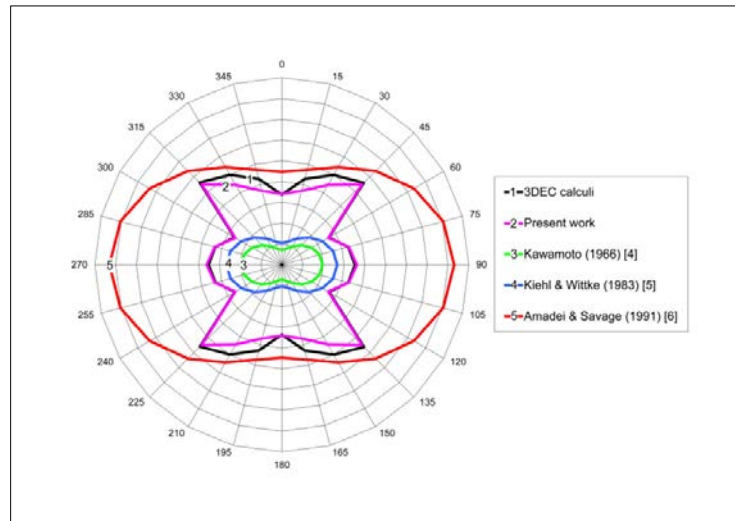


Fig. 15. Comparison of different equations for deformation of a cylindrical cavity with  $\beta=90^\circ$ .

#### 4. Conclusions

From this study we can conclude:

- The presence of discontinuity planes is the principal source of anisotropy in most of the rock masses. The deformability and spacing of these planes ( $k_n$ ,  $k_s$ , and  $\lambda$ ) greatly influence the deformability of the rock mass.
- The deformability of a rock mass is a complex issue. This fact gets more complicated in a jointed and anisotropic rock mass.
- The use of pressuremeter tests (or similar ones) is an inexpensive and an easy way to measure the deformability; however, its habitual interpretation supposes a continuous and isotropic medium.
- Some methods for the interpretation of cavity expanding tests in anisotropic media have been published, but none of them takes into account the slide of joints. Here, we propose a new method that considers this phenomenon.
- A critical dip angle of the discontinuity ( $\chi$ ) has been observed. When the dip angle of the joints ( $\beta$ ) is greater than  $\chi$ , the slide of the joints occurs and a continuum medium interpretation is useless.
- The model proposed allows the estimation of the deformability of a jointed rock mass, for any dip angle of the discontinuity planes, from the analysis of pressuremeter tests.

#### Acknowledgements

We want to acknowledge to our colleague Dr. Javier Moreno Robles his advice in the developing of the numerical models. We also want to acknowledge Ms. Raquel Fuertes, MSc. her reviews of the text.

#### References

- [1] A. Serrano, C. Olalla, A. Perucho, Evaluation Of Non-Linear Strength Laws For Volcanic Agglomerates, in: C. Dinis da Gama, L. Ribeiro e Sousa (Eds.), ISRM International Symposium - EUROCK 2002, International Society for Rock Mechanics, Madeira, Portugal, 2002.
- [2] M. Romana, Determination of deformation modulus of rock masses by means of geomechanical classification, in: Proceedings of EUROCK'02 international symposium, Sociedade Portuguesa de Geotecnia, Madeira island, Portugal, 2002, pp. 317-325.
- [3] N. Barton, Model study of rock-joint deformation, Int. J. Rock Mech. Min. Sci. 9 (1972) 579-&.
- [4] T. Kawamoto, On the Calculation of the Orthotropic Elastic Properties From the States of Deformation Around a Circular Hole Subjected to Internal Pressure In Orthotropic Elastic Medium, in: 1st ISRM Congress, LNEC (National Laboratory for Civil Engineering), Lisbon, Portugal, 1966.



- [5] J.R. Kiehl, W. Wittke, Determination of the deformability of anisotropic rocks from the results of field tests (in German), in: 5th ISRM Congress, Australian Geomechanical Society, Melbourne, Australia, 1983.
- [6] B. Amadei, W.Z. Savage, Analysis of borehole expansion and gallery tests in anisotropic rock masses, *Int. J. Rock Mech. Min.* 28 (1991) 383-396.
- [7] D. Kolymbas, P. Wagner, A. Blioumi, Cavity expansion in cross-anisotropic rock, *Int. J. Numer. Anal. Met.* 36 (2012) 128-139.
- [8] A.M. Hefny, K.Y. Lo, Analytical solutions for stresses and displacements around tunnels driven in cross-anisotropic rocks, *Int. J. Numer. Anal. Met.* 23 (1999) 161-177.
- [9] P. Fortsakis, K. Nikas, V. Marinos, P. Marinos, Anisotropic behaviour of stratified rock masses in tunnelling, *Eng. Geol.* 141 (2012) 74-83.
- [10] T.T. Wang, T.H. Huang, Anisotropic Deformation of a Circular Tunnel Excavated in a Rock Mass Containing Sets of Ubiquitous Joints: Theory Analysis and Numerical Modeling, *Rock Mech. Rock Eng.* 47 (2013) 643-657.
- [11] Singh, M., Singh, B., Choudhari, J. B., Goel, R. K., Constitutive equations for 3-D anisotropy in jointed rocks and its effect on tunnel closure, *Int. J. Rock Mech. Min.* 41 (2004) 652-657.
- [12] M. Muñiz Menéndez, Geotechnical Units of the future Fix Link between Europe and Africa under the Strait of Gibraltar (in Spanish), Ph.D. Thesis, Complutense University, Madrid, 2015, pp. 477.
- [13] Itasca Consulting Group, I., 3 Dimensional Distinct Element Code. 3DEC 4.1 Theory and Manual, Minneapolis, USA, 2011.